Weather and Climate Extremes 35 (2022) 100407

Contents lists available at ScienceDirect

Weather and Climate Extremes

journal homepage: www.elsevier.com/locate/wace

Characterizing extreme values of precipitation at very high resolution: An experiment over twenty European cities

A. Reder *, M. Raffa, R. Padulano, G. Rianna, P. Mercogliano

Regional Models and Geo-Hydrological Impacts (REMHI) Division, Fondazione Centro Euro-Mediterraneo sui Cambiamenti Climatici, Via T. A. Edison, 81100, Caserta, Italy

ARTICLE INFO

Keywords:
Dynamical downscaling
Climate reanalysis
ERA5 reanalysis
Convection permitting scale
IDF curves
Sub-daily extreme rainfall
Disaster risk reduction

ABSTRACT

The paper presents a new hourly high-resolution (i.e., at 0.02°, ≃2.2 km) precipitation dataset, labelled as ERA5@2km, obtained by dynamically downscaling ERA5 reanalysis at convection permitting scale (CPS) over 20 European cities for the recent past thirty years (1989–2018). The downscaling activity is performed within the framework of the Contract implemented by Fondazione CMCC to support Sectoral Information System about "Disaster Risk Reduction" (see https://climate.copernicus.eu/pluvial-flood-risk-assessment-urban-areas) of Copernicus Climate Change Service (C3S). Specifically, such an additional precipitation dataset is developed to provide precipitation data for estimating expected precipitations at fixed return periods used as input for pluvial flooding risk analysis where hazard (inundated areas, water levels) and risk (estimated damages) are assessed. The ambition is to support the Disaster Risk Reduction (DRR) community involved in pluvial flood risk assessment by providing a basis for impact analysis at city scale, in terms of extreme hourly precipitation, that matches with the expected spatial and temporal requirements. In this work, ERA5@2km precipitation dataset is introduced for the first time and its reliability and coherence are evaluated as for spatial patterns and trends as for extreme values against a set of available high-resolution observational datasets (comparable in terms of spatial and temporal resolution). Such an evaluation provides a clearer understanding about the added value of very high-resolution (VHR) dynamical downscaling reanalysis in terms of localization and magnitude of precipitation events at urban scale, confirming a general and relevant added value of this new configuration for the assessment of extreme atmospheric events (such as heavy precipitations).

1. Introduction

The availability of homogeneous and continuous data (in terms of time and space) represents a key requirement for characterizing extreme past weather events and the associated physical and socio-economic impacts (Street et al., 2019). Their spatial and temporal resolution regulate indeed both the dynamics that could be properly investigated and the limitations to account for their use.

In this regard, the most obvious support is represented by in-situ weather station measurements. However, they are rarely available over long time spans, and often outline a scarce homogeneity and density of observation points which are assumed as reference for large areas, despite such a constrain. To cope with such limitations, in recent years several gridded observational datasets have been developed for Europe (e.g., E-OBS, Cornes et al., 2018) and for specific European countries, e.g., SAFRAN (Vidal et al., 2010) and COMEPHORE (Tabary et al., 2012) for France, PTHBV (Johansson, 2000) for Sweden, HYRAS (Rauthe et al., 2013; Frick et al., 2014) and RADKLIM-RW (Winterrath et al., 2018) for Germany; seNorge2 (Lussana et al., 2018) for Norway, TabsD (MeteoSwiss, 2013a) and RhiresD (MeteoSwiss, 2013b) for Switzerland, CEH-GEAR (Lewis et al., 2019) for Great Britain, SCIA-ISPRA (Desiato et al., 2011) and GRIPHO (Fantini, 2019) for Italy, IBERIA01 (Herrera et al., 2019) for Iberian Peninsula. These products feature different temporal (e.g., from hourly to daily) and spatial (e.g., from ≃ 1 km to ≃ 10–20 km) resolutions, covering different time spans; in addition, their reliability is strictly related to the density of station networks from which they derive.

A potential alternative solution to ensure homogeneity and continuity of data is represented by the use of climate reanalysis. In general, a climate reanalysis "delivers a complete and consistent picture of the past weather" (https://youtu.be/FAGobvUGl24) by adopting a numerical weather prediction model to assimilate historical observations provided

* Corresponding author.
E-mail address: alfredo.reder@cmcc.it (A. Reder).

https://doi.org/10.1016/j.wace.2022.100407
Received 27 April 2021; Received in revised form 12 October 2021; Accepted 17 January 2022
Available online 20 January 2022

by different sources (satellite, in situ, multiple variables) but not homogeneously distributed around the globe. Recently, the European Centre for Medium Range Weather Forecast (ECMWF) has released a new generation of reanalysis, acknowledged as ERA5, representing nowadays the most plausible description for current climate (Hersbach et al., 2020). It has a global coverage with a spatial resolution of 0.25° (≃ 31 km) and provide outputs at hourly scale since 1950 up to now (with a latency of 5 days). Such features make ERA5 suitable for a wide range of applications such as monitoring climate change, research, education, policy making and business, in sectors such as renewable energy and agriculture (Buontempo et al., 2020). It forms the basis for monthly C3S climate bulletins and is used in the World Meteorological Organization's annual assessment of the State of the Climate presented at the Conference of the Parties of the United Nations Framework Convention on Climate Change (UNFCCC). In addition to ERA5, other advanced reanalysis products recently released are ERA5-Land (Muñoz-Sabater et al., 2021) and UERRA (Ridal et al., 2017). The former represents a refined version of ERA5 for land variables with a spatial resolution of ≃ 9 km; the latter is a refined version of ERA40/ERA-Interim (Dee et al., 2011) reanalysis over Europe at ≃ 5.5 km providing however precipitation at daily scale.

Despite the authoritative relevance of ERA5, its coarse resolution could prevent a reliable adoption for characterizing localized events (e.g., extreme precipitation) in special way in complex areas (e.g., mountain or urban environments). In this perspective, the ongoing developments of convection-permitting regional climate models (CP-RCMs, resolution <4 km) are providing a possible solution to partly cover this gap. CP-RCMs represent a step change in the capability for understanding past climate and future climate change at local scales and for extreme weather events that most impact society (Kendon et al., 2021). This includes credible data for short-duration precipitation extremes, as CP-RCMs resolution avoids the use of error-prone deep convection parameterization schemes, responsible in some cases of a misinterpretation of precipitation patterns and trends.

Some European initiatives (e.g., H2020 EUCP, see https://www.eucp-project.eu/, CORDEX-FPS convection, see https://www.hymex.org/cordexfps-convection/wiki/doku.php), and an increasing number of scientific works (e.g., Ban et al., 2014; Berthou et al., 2018; Coppola et al., 2020; Fumière et al., 2020; Reder et al., 2020; Fosser et al., 2015; Prein et al., 2015; Piazza et al., 2019; Adinolfi et al., 2021; Raffa et al., 2021; Ban et al., 2021) are providing a reference baseline to demonstrate the added value of this specific configuration. Such an improvement can be noted in a more accurate representation of some features, e.g., the diurnal cycles, hourly precipitation intensities, local–regional circulations, seasonal average precipitation, convective downdrafts, and the representation of cold pools (Coppola et al., 2020; Fowler et al., 2021; Ban et al., 2021). All these insights are encouraging the climate community to deeply investigate the potential added values of CP-RCMs for a more adequate representation of climate condition over urban areas, especially for the extremes.

Investigations about potentialities of such approaches for impact studies at very high resolution (VHR) represent one of the outputs of the Contract implemented by Fondazione CMCC to support Sectoral Information System about "Disaster Risk Reduction" (see https://climate.copernicus.eu/pluvial-flood-risk-assessment-urban-areas) of Copernicus Climate Change Service (C3S). Specifically, an experiment to downscale ERA5 at CP scale (i.e., at 0.02°, ≃2.2 km) is carried out over 20 European cities to obtain a high-resolution hourly precipitation dataset (ERA5@2km) for the recent past thirty years (1989–2018). Such data are then adopted as inputs for estimating expected precipitations at fixed return periods (see Annex B) and used as input for a tailored pluvial flooding risk analysis. The ambition is to support the Disaster Risk Reduction (DRR) community involved in pluvial flood risk assessment by providing a basis for impact analysis at city scale, in terms of extreme hourly precipitation, that matches with the expected spatial and temporal requirements.

In this work, ERA5@2km precipitation dataset is introduced for the first time. Its reliability and coherence are evaluated as for spatial patterns and trends as for extreme values against a set of available high-resolution observational datasets (comparable in terms of spatial and temporal resolution). Such an evaluation provides a clearer understanding about the added value of very high-resolution (VHR) dynamical downscaling reanalysis in terms of localization and magnitude of precipitation events at urban scale confirming a general and relevant added value of this new configuration for the assessment of extreme atmospheric events (such as heavy precipitations).

The paper first describes (§2) the experimental setup (§2.1) with the observational datasets (§2.2) considered for the evaluation. Then, it introduces the statistical tools used for the evaluation (§2.3) and for obtaining extreme hourly precipitation at prescribed recurrence intervals (§2.4). Finally, it presents (§3.1 and §3.2) the new precipitation dataset at city scale by assessing its performance against observational datasets at different temporal and spatial resolutions.

2. Material and methods

2.1. Climate experiment

ERA5 is dynamically downscaled at convection permitting scale (0.02°, ≃2.2 km) to derive a high-resolution hourly precipitation dataset, labelled as ERA5@2km, over a pool of 20 European cities for the 30-years period 1989–2018. The downscaling is performed with the Regional Climate Model (RCM) COSMO-CLM (CCLM) (Rockel et al., 2008) switching on the module TERRA-URB (Wouters et al., 2016) for accounting for the urban parameterizations.

Fig. 1 displays the analysis domains used for the downscaling activity. Specifically, nine domains are defined to optimize the simulations over the 20 cities according to the standard prescriptions reported in Prein et al. (2015) for the selection of domain size.

Table 1 summarizes the main features of the climate experiment, listing the parameterizations used to account for the sub-grid-scale physical processes.

This configuration relies on the optimized COSMO-DE setup, resulting from the protocol established in the framework of the Coordinated Downscaling Experiment (CORDEX) (Giorgi et al., 2015; Jacob et al., 2014) of the World Climate Research Programme (WCRP) for the Flagship Pilot Study (FPS) on convection (Coppola et al., 2020). Such an FPS focuses on the investigation of convective-scale events in a few key regions of Europe and the Mediterranean basin with convection-permitting regional climate models.

Formally, the default COSMO convective parameterization is the Tiedtke mass-flux scheme with moisture-convergence closure (Tiedtke, 1989). Such a scheme distinguishes between shallow, deep, and mid-level convection. In the convection-resolving setup (i.e., that used for ERA5@2km), only the shallow convection part of the scheme is active, while for deeper clouds the scheme is turned off.

The setup reported in Table 1 was also borrowed from the ERA5 evaluation downscaling experiments performed by Raffa et al. (2021) over part of central Europe, including some cities such as Cologne (Germany) and Paris (France). These experiments were performed to identify the most reliable nesting strategy to be adopted for localizing ERA5 climate signal at convection permitting scale (≃2.2 km) with CCLM in the view of deriving precipitation characteristics at city scale or at the event scale. Specifically, Raffa et al. (2021) tested two nesting strategies: the former, labelled as "CCLM002-Direct", relying on a one-step nesting strategy in which the simulation at 2.2 km is directly "one-way nested" in ERA5 (1:15 resolution jump); the latter, labelled as "CCLM002-Nest", considering a "two-step nesting strategy" in which the simulation at 2.2 km is one-way nested in a 12 km grid spacing which in turn is one-way nested in ERA5 (1:3:6 resolution jump). The Authors pointed out that CCLM002-Direct outperforms CCLM002-Nest if it is evaluated at the city scale or at the event scale. This tendency was

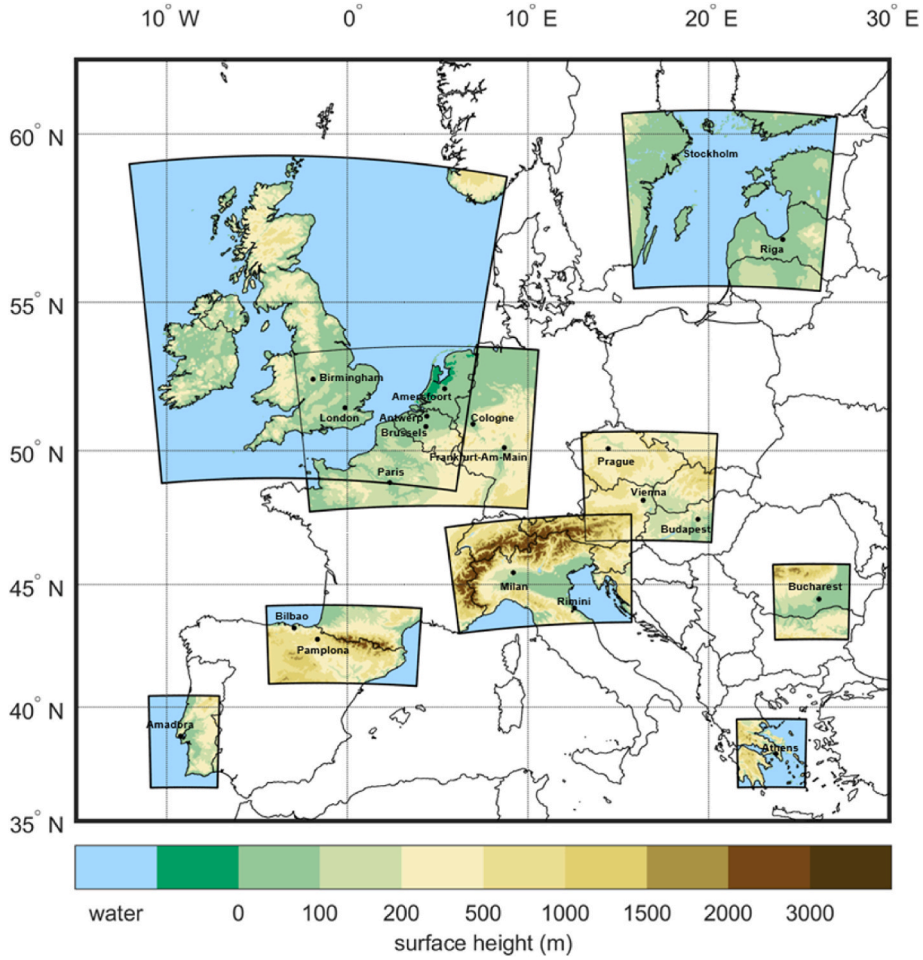

Fig. 1. Analysis domains defined for the downscaling activity.

Table 1
Main characteristics of the experiment configurations (Raffa et al., 2021).

Model	ERA5@2km
Boundary forcing	ERA5-Reanalysis
Horizontal resolution	0.02° (≃2.2 km)
Time step	20 s
N° grid points	Variable (depending on the considered computational domain)
N° vertical levels	50
Output frequency	1 h
Temporal coverage	1989–2018 (1988 as spin up)
Radiation scheme	Ritter and Geleyn (1992)
Convection scheme	Shallow convection based on Tiedtke (1989)
Microphysics scheme	Doms et al. (2011); Baldauf and Schulz (2004)
Land surface scheme	TERRA-ML (Doms et al., 2011) with TERRA-URB (Wouters et al., 2016) parametrization
Land use	GLC2000 (Bartholomé and Belward, 2005)
Planetary boundary layer scheme	Mellor and Yamada (1982)
Lateral Boundary Condition (LBC) update frequency	1 h
Soil initializations	Temperature and moisture obtained by interpolation from ERA5-Reanalysis

ascribed to the fact that CCLM002-Nest is driven at the Lateral Boundary Condition (LBC) by a freely evolving (i.e., not nudged) intermediate simulation allowing internal variability to develop (Coppola et al., 2020). For this reason, events at the meteorological scale and over a very limited area of interest could not be correlated with ERA5. Conversely, such a tendency seems to be attenuated when CCLM002 is directly nested into ERA5. For this reason, in this study ERA5@2km is directly "one-way nested" in ERA5 to ensure reliability, coherence, and consistency as for climate statistics as for limited area and periods.

Operatively, ERA5 data are firstly pre-processed to be adapted for CCLM simulation within the CCLM community, with the support of HZG and DWD. The pre-processed data are then used as input for the interpolation pre-processor (INT2LM) to generate the initial and boundary conditions on the ERA5@2km grid. Finally, a long-term climate simulation is performed implementing an automatic restart procedure to avoid potential interruptions of simulation.

2.2. Observational datasets

High-resolution observational precipitation datasets available over different areas at hourly scale are considered to evaluate the reliability and coherence of precipitation data provided by ERA5@2km at city scale. These datasets are selected to be as comparable as possible in terms of spatial and temporal resolution against ERA5@2km. Specifically:

- CEH-GEAR (Lewis et al., 2019): it is an hourly gridded precipitation dataset for Great Britain at a horizontal resolution of 1 km for the period 1990–2014, derived by temporally disaggregating the CEH-GEAR daily precipitation dataset according to a national database of hourly rain gauge observations.
- RADKLIM-RW (Winterrath et al., 2018): it is a radar-based dataset, available at the DWD Open Data Portal, providing hourly

precipitation adjusted to rain gauge measurements for Germany at a horizontal resolution of 1 km for the period 2001–2017.
- GRIPHO (Fantini, 2019): it is an hourly gridded precipitation dataset for Italy, based on rain gauge measurements, at a horizontal resolution of 10 km for the period 2001–2016.

In addition, to perform a general evaluation overview for those cities for which hourly gridded observations are not available in our knowledge, a daily observational precipitation dataset is considered. Specifically:

- E-OBS (Cornes et al., 2018; Haylock et al., 2008): it is a daily gridded land-only observational dataset over Europe at a horizontal resolution of 0.1° (≃11 km) for the period 1950–2020, containing data for precipitation amount, mean/maximum/minimum temperature, sea level pressure, and surface shortwave downwelling radiation. E-OBS relies on the blended time series from the station network of the European Climate Assessment & Dataset (ECA&D) project. It is calculated following a two-stage process to derive the daily field and the uncertainty in these daily estimates.

Observational precipitation gridded datasets could feature some constraints and limitations (Isotta et al., 2014; Adinolfi et al., 2021). In general, a grid point is informative for an area, depending on the spatial resolution of the considered gridded dataset. For each grid cell, precipitations could be affected in their magnitude by an averaging effect; then, the coarser the spatial resolution the larger the smoothing effect. Additional issues are: (i) precipitation underestimation at high elevation due to the not properly accounted precipitation lapse rate and that induced by stations sparseness and mask-effect issues for radar data; (ii) systematic wind-induced rain gauge under-catch, and (iii) wetting and evaporation losses; (iv) interpolation methods, which systematically induce underestimation of high intensities (smoothing effect) and overestimation of low intensities (moist extension into dry areas).

The effect of these limitations and constraints tends to decrease with spatial resolution (e.g., for RADKLIM-RW, and CEH-GEAR). However, for these datasets, a further source of uncertainty is represented by the methods adopted to merge rain gauge measurements and radar data as well as by the use of statistical disaggregation approaches. Regarding E-OBS, it builds on the ECA&D station network, whose diverse coverage over Europe makes such a dataset more reliable in some regions than in others (Cornes et al., 2018).

2.3. Evaluation metrics

Precipitation data provided by ERA5@2km at city scale are assessed with respect to available observational datasets by using a set of widely adopted indices for performance evaluation, namely KGE (Kling–Gupta Efficiency, Gupta et al., 2009), and DAV (Distribution Added Value, Soares and Cardoso, 2017); the same indices are also adopted for deriving the potential added value of ERA5@2km with respect to the parent ERA5 reanalysis.

KGE is a goodness-of-fit measure for evaluating the performance of a model time-series (subscript m) with respect to an observed one (subscript *obs*):

$$\mathrm{KGE} = 1 - \sqrt{(\rho - 1)^2 + \left(\frac{\sigma_m}{\sigma_{obs}} - 1\right)^2 + \left(\frac{\mu_m}{\mu_{Obs}} - 1\right)^2} \quad (1)$$

where ρ is the Pearson correlation coefficient data, σ represents the standard deviation, and μ is the mean. KGE = 1 indicates a perfect agreement between observed and simulated data; KGE < −0.41 indicates that model data underperform the mean of observed data (Knoben et al., 2019).

DAV provides an objective and normalized measure of the added value in terms of potential gain in the performance of climate models due to the usage of a higher resolution, comparing higher- and coarser-resolution simulation probability density function (PDFs) to the observational PDF. DAV accounts for the difference in skill scores (Perkins et al. 2007) between high resolution (subscript *hr*) and low resolution (subscript *lr*) assuming the observations (subscript *obs*) as reference:

$$DAV = \frac{S_{hr} - S_{lr}}{S_{lr}} = \frac{\sum_1^n \min(Z_{hr}, Z_{obs}) - \sum_1^n \min(Z_{lr}, Z_{obs})}{\sum_1^n \min(Z_{lr}, Z_{obs})} \quad (2)$$

where S_{hr} and S_{lr} are the Perkins skill scores for high and low resolution respectively; n is the number of bins considered to obtain the PDF; Z_{hr}, Z_{lr} and Z_{obs} are the frequencies of values in each bin for high resolution, low resolution, and observations respectively. In general, DAV = 0 indicates that no gain is found; DAV <0 points out a loss associated to the usage of a higher resolution; DAV >0 expresses the beneficial impact of increasing the grid spacing.

Both KGE and DAV are computed at city scale considering the evaluation domains reported in Table 2.

With the precise intent of avoiding artificial downscaling/upscaling and emphasizing the actual added value at a finer scale, data are not interpolated over a common grid.

2.4. Intensity-duration-frequency (IDF) curves at city scale

To interpret extreme precipitation values and to obtain annual maximum hourly precipitation at prescribed recurrence intervals, the storm index method (Viglione et al., 2007; Padulano et al., 2019) is adopted.

According to the storm index method, the rainfall depth of an extreme precipitation event x with return period T and rainfall duration d can be estimated (Eq. (3)) as the product of a scale parameter (μ) only depending on duration d (i.e., deterministic part of Eq. (3)), and a frequency parameter or "growth factor" (k_T) only depending on the return period T (i.e., probabilistic part of Eq. (3)):

$$x(d, T) = \mu[x(d)] \cdot k_T(T) \quad (3)$$

Eq. (3) is known to ensure rainfall consistency, as it preserves the increasing dependence of precipitation depth on both duration and return period. Moreover, in practical applications, Eq. (3) is often subject to a regionalization process whose aim is to identify homogeneous areas (usually related to significant hydrographic units such as watersheds) where the statistical behaviour of extreme rainfall can be considered the same, and relations are calibrated basing on pooled samples (Wallis et al., 2007). In this perspective, within a homogeneous region only one probability model is calibrated, whereas mean rainfall is considered spatially distributed (implying a possible dependence on elevation z as well as on duration d). The use of a pooled sample is the cornerstone of regional frequency analysis of extreme rainfall events, positively including a larger number of extreme rainfall events and increasing the statistical significance and reliability of evaluations (Caporali et al., 2008; Madsen et al., 2017).

In the paper, prior to pooling, the homogeneous behaviour of rainfall data is inspected and ensured for both components of the storm index method by suitable statistical testing, such as the one-way ANOVA test (Kottegoda and Rosso, 2008) and the Anderson-Darling test (Anderson and Darling, 1954).

In the following, the procedure applied at city scale to calibrate Eq. (3) is described:

1) for each grid point, the hourly precipitation amounts are first aggregated with a fixed-width moving window for six reference durations d (1, 2, 3, 6, 12 and 24 h); from these six samples of precipitation, the annual maximum rainfall depths (AMR) are then extracted to obtain six AMR samples;
2) the different AMR samples are subjected to hypothesis tests (Kottegoda and Rosso, 2008; Anderson and Darling, 1954) to check

Table 2
Spatial delimitation (in terms of Longitude and Latitude) of the evaluation domains at city scale; each city domain is centred on the relative NUTS 3 (Nomenclature of Territorial Units for Statistics at third level).

City	NUTS 3	Boundary Box
Amadora (Portugal)	PT170 –Lisboa	Lon = 9.75°W – 8.25°W Lat = 38.25°N – 39.25°N
Amersfoort (the Netherlands)	NL310 – Utrecht	Lon = 4.5°E – 5.75°E Lat = 51.75°N – 52.5°N
Antwerp (Belgium)	BE211 – Arr. Antwerpen	Lon = 4°E – 5°E Lat = 51°N – 51.75°N
Athens (Greece)	EL301 – Northern Athens; EL302 – Western Athens; EL303 – Central Athens; EL304 – Southern Athens	Lon = 23.5°E – 24°E Lat = 37.75°N – 38.25°N
Bilbao (Spain)	ES213 – Bizkaia	Lon = 3.5°W – 2.25°W Lat = 42.75°N – 43.75°N
Birmingham (United Kingdom)	UKG31 – Birmingham	Lon = 2.3°W – 1.25°W Lat = 52.25°N – 52.75°N
Brussels (Belgium)	BE100 – Arr. de Bruxelles-Capitale/ Arr. van Brussel-Hoofdstad	Lon = 4°E – 4.75°E Lat = 50.5°N – 51.25°N
Bucharest (Romania)	RO321 – Bucuresti	Lon = 25.75°E – 26.5°E Lat = 44.25°N – 44.75°N
Budapest (Hungary)	HU110 – Budapest	Lon = 18.75°E – 19.5°E Lat = 47.25°N – 47.75°N
Cologne (Germany)	DEA23 – Koln, Kreisfreie Stadt	Lon = 6.5°E – 7.5°E Lat = 50.75°N – 51.25°N
Frankfurt Am Main (Germany)	DE712 – Frankfurt am Main, Kreisfreie Stadt	Lon = 8.25°E – 9°E Lat = 49.75°N – 50.5°N
London (United Kingdom)	UKI41 – Hackney and Newham; UKI42 – Tower Hamlets; UKI43 – Haringey and Islington; UKI44 – Lewisham and Southwark; UKI45 – Lambeth; UKI31 – Camden and City of London; UKI32 – Westminster	Lon = 0.75°W – 0.5°E Lat = 51°N – 52°N
Milan (Italy)	ITC4C – Milano	Lon = 8.5°E – 9.75°E Lat = 45°N – 45.75°N
Pamplona (Spain)	ES220 – Navarra	Lon = 2.75°W – 0.5°W Lat = 41.75°N – 43.5°N
Paris (France)	FR101 – Paris; FR105 – Hauts-de-Seine; FR106 – Seine-Saint-Denis; FR107 – Val-de-Marne	Lon = 2°E – 2.75°E Lat = 48.5°N – 49.25°N
Prague (Czech Republic)	CZ010 – Praha	Lon = 14°E – 15°E Lat = 49.75°N – 50.5°N
Riga (Latvia)	LV006 – Riga	Lon = 23.75°E – 24.5°E Lat = 56.75°N – 57.25°N
Rimini (Italy)	ITH59 – Rimini	Lon = 12°E – 13°E Lat = 43.5°N – 44.25°N
Stockholm (Sweden)	SE110 – Stockholms County	Lon = 17°E – 19.75°E Lat = 58.5°N – 60.5°N
Vienna (Austria)	AT130 – Wien	Lon = 16°E – 16.75°E Lat = 48°N – 48.5°N

whether extreme data related to different points of a domain of interest can be considered extracted from the same population (in terms of mean values, growth factors, or both) and then pooled together to build robust calibration of Eq. (3);

3) for the scale parameter μ (depending on elevation z as well as on duration d), the model proposed by Sherman (Chow et al., 1988) is adopted and calibrated:

$$\mu[x(d,z)] = \frac{A \cdot d}{(C+d)^{(B+D \cdot z)}} \tag{4}$$

the goal of such a calibration procedure is to determine the set of parameters (i.e., A, B, C, D);

4) for the growth factor k_T (only depending on the return period T), the Generalized Extreme Value (GEV) probability distribution model (Hosking et al., 1985), whose Probability Density Function (PDF) can be expressed by the following equation, is adopted and calibrated:

$$f(k,\sigma,\mu) = \left(\frac{1}{\sigma}\right) \cdot exp\left\{ -\left[1 + k \cdot \frac{(x-\mu)}{\sigma}^{-\frac{1}{k}}\right]\right\}\left[1 + k \cdot \frac{(x-\mu)}{\sigma}\right]^{-1-\frac{1}{k}} \tag{5a}$$

$$f(0,\sigma,\mu) = \left(\frac{1}{\sigma}\right) \cdot exp\left\{ -exp\left[-\frac{(x-\mu)}{\sigma}\right] - \frac{(x-\mu)}{\sigma}\right\} \tag{5b}$$

the goal of such a calibration procedure is to determine the set of GEV parameters (i.e., shape k, scale σ, location μ). The calibration procedure is applied on the pooled AMR sample normalized by its mean value. In this way, a pooled dimensionless sample is obtained.

3. Results and discussion

3.1. Validation against high resolution observational datasets

The first part of the study consists in evaluating precipitation data provided by ERA5@2km with respect to high-resolution hourly observational precipitation datasets (i.e., CEH-GEAR, RADKLIM-RW, and GRIPHO). At the same time, it is also considered the parent ERA5 reanalysis to investigate the potential added value arising from the use of ERA5@2km data. Such an evaluation is performed over a subset of 20 European cities for which ERA5@2km data are provided. Specifically, CEH-GEAR data are adopted for London (UK); RADKLIM-RW data for Cologne (DE); GRIPHO data for Milan (IT). For Cologne, such an evaluation represents an extension with respect to the analyses reported in Raffa et al. (2021) as for the time windows considered as for type of analyses.

For each dataset, the observational periods overlapping with the targeted simulation period are considered. This is 1990–2014 for CEH-GEAR data, 2001–2017 for RADKLIM-RW data, and 2001–2016 for GRIPHO data. These periods can be considered long enough for evaluation analyses.

For each city, precipitation data are evaluated at different temporal scales (from annual to hourly) as well as for both average patterns and extremes. The aim is to highlight the benefits due to the dynamical downscaling of ERA5 at convection permitting scale. Specifically, the following issues are analysed:

- the spatial pattern of mean annual precipitation
- the multi-year cycle of monthly precipitation
- the probability density function (PDF) of hourly precipitation; it is defined as the normalized frequency of occurrence of precipitation events within a certain bin
- the multi-year cycle of hourly precipitation for summer season (JJA = June-July-August) to focus on convective events that are known to be more frequent in this season than non-convective ones
- the annual maximum hourly precipitation at prescribed recurrence intervals (i.e., 5-10-25-50-100 y)

Synthetical indices are adopted for the different analysis to quantify gains and losses associated with the use of VHR simulations.

For all the cities reported in Table 2, Annex A shows spatial distribution of annual precipitation provided by E-OBS, ERA5, and ERA5@2km as well as the multi-year cycle of monthly precipitation and the annual maximum daily precipitation at prescribed return periods. For the latter, the daily scale is considered to compare hourly dataset with E-OBS data; moreover, annual maximum daily precipitations at prescribed return periods relying on ECA&D station network (Mercogliano et al., 2021) and included in the Copernicus Climate Data Store

(CDS) are used as additional reference. They are computed starting from local weather station precipitation data and then interpolated onto the E-OBS grid. Further details about the procedure used for their computation are reported in the Product User Guide associated to the Dataset. Finally, Annex B reports an overview of IDF parameters (Eq. (4) and Eq. (5)) obtained interpreting annual maximum precipitation provided by ERA5@2km over for the 20 European cities.

3.1.1. Validation against CEH-GEAR (1990–2014) for London (UK)

Fig. 2 shows the spatial distribution of annual precipitation provided by ERA5 (Fig. 2a), ERA5@2km (Fig. 2b) and CEH-GEAR (Fig. 2c) for London (UK). The maps are plotted considering all the grid points belonging to the city evaluation domains in their native resolution (i.e., 16, 1386, and 6256 grid points for ERA5, ERA5@2km, and CEH-GEAR, respectively).

Observational dataset CEH-GEAR (Fig. 2c) returns values with a spatial average of 669 mm/y and a spatial standard deviation of 68 mm/y. Compared to the reference observations, ERA5@2km (Fig. 2b) slightly increases annual precipitation in terms of spatial averages (= 691 mm/y) with a reduced spatial variability (standard deviation = 30 mm/y). From a spatial viewpoint, it well detects areas characterized by higher values of annual precipitation as for observations, even if peaks are lowered (also due to the coarser resolution). Finally, ERA5 (Fig. 2a) returns the highest spatial average of annual precipitation (= 703 mm/y) and the lower spatial variability (standard deviation = 26 mm/y) with respect to the other cases; moreover, despite its coarser resolution, ERA5 roughly identifies rainy areas.

The multi-year cycle of monthly precipitation is plotted in Fig. 3 for the same datasets considered for Fig. 2.

CEH-GEAR monthly precipitation ranges in-between 38 mm/month and 73 mm/month with minimum value in March and maximum values in October and November. Compared to CEH-GEAR, ERA5 detects minimum and maximum peaks even if these latter are lowered; moreover, monthly precipitation from April to August is overestimated. Enhancing the spatial resolution with ERA5@2km removes such an overestimation and increases the maximum values, returning a trend in line with CEH-GEAR. Such an improvement also arises in terms of KGE (Eq. (4)) calculated by considering monthly precipitation over the investigated period for both ERA5 (KGE = 0.85) and ERA5@2km (KGE = 0.92) over 1990–2014, assuming CEH-GEAR as reference.

Moving to the hourly scale, Fig. 4 shows the PDFs of hourly precipitation provided by CEH-GEAR, ERA5, and ERA5@2km.

CEH-GEAR hourly precipitation PDF returns a tail with maximum value of ≃ 9 mm/h. Compared to observations, the models' hourly

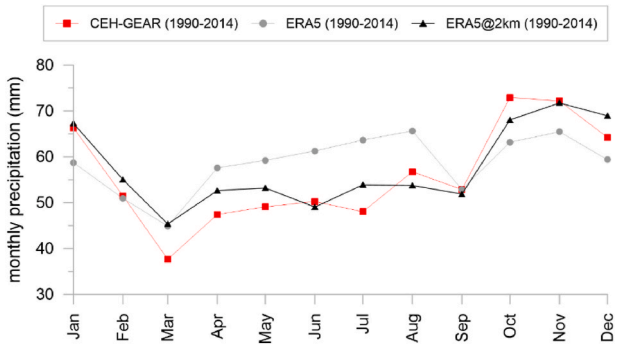

Fig. 3. Annual cycle of monthly precipitation over London (UK) for the period 1990–2014 with different datasets (i.e., CEH-GEAR, ERA5, ERA5@2km).

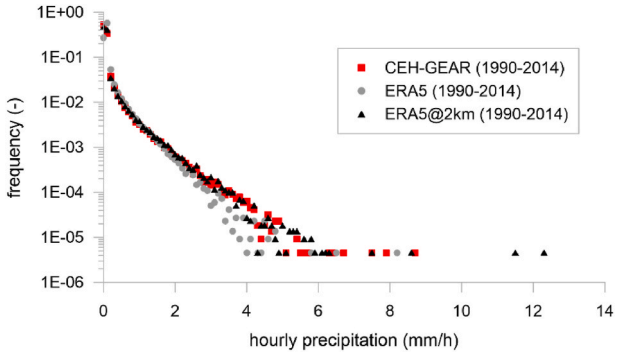

Fig. 4. Probability density function (PDF) of hourly precipitation over London (UK) for the period 1990–2014 with different datasets (i.e., CEH-GEAR, ERA5, ERA5@2km).

precipitation PDFs detect an underestimation by the coarser resolution model (i.e., ERA5) for hourly precipitation values in the range 3–5 mm/h, while the new dataset ERA5@2km returns values closer to observations, with a tendency to produce a longer tail (≃ 12 mm/h). By applying the DAV metric on the hourly precipitation PDFs, it is possible to quantify a gain (DAV = 21%) associated with the use of ERA5@2km with respect to ERA5.

Fig. 5 compares the multi-year cycle of hourly summer precipitation provided by CEH-GEAR, ERA5, and ERA5@2km.

CEH-GEAR returns a cycle of hourly precipitation that is typical of

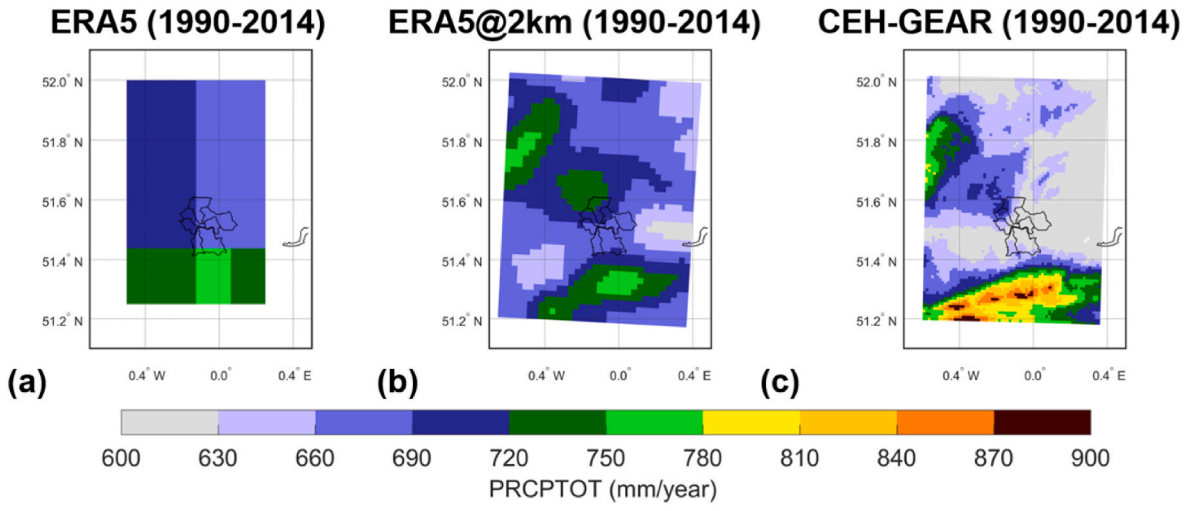

Fig. 2. Average annual precipitation over London (UK) for the period 1990–2014 with different datasets: (a) ERA5 (≃ 31 km); (b) ERA5@2km (≃ 2.2 km); (c) CEH-GEAR (≃ 1 km).

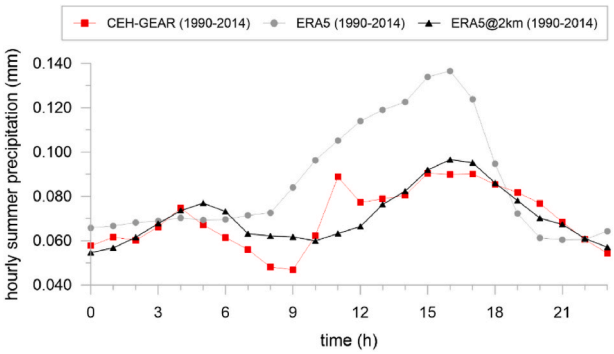

Fig. 5. Daily cycle of hourly summer precipitation over London (UK) for the period 1990–2014 with different datasets (i.e., CEH-GEAR, ERA5, ERA5@2km); time is in UTC.

the summer period, with higher values in the afternoon despite a discontinuity at 11UTC. Such a discontinuity should require further investigations. ERA5 well detects the same cycle provided by CEH-GEAR; however, it significantly overestimates the amplitude of hourly precipitation during the daylight hours (from 9UTC to 18UTC) with values up to 0.137 mm/h (peak at 16UTC). ERA5@2km reduces such an overestimation returning a trend like CEH-GEAR; its peak occurs at 16UTC (synchronous to ERA5), but the amplitude (=0.095 mm/h) matches observations. In terms of KGE, ERA5@2km significantly outperforms ERA5 (KGE = 0.04 for ERA5 against KGE = 0.77 for ERA5@2km).

Finally, to assess ERA5@2km performance in terms of extreme precipitation, Fig. 6 compares the annual maximum hourly precipitation computed at prescribed recurrence intervals by ERA5@2km with those provided by CEH-GEAR and ERA5 (Fig. 5c). For all the datasets, the procedure outlooked in Section 3.2 is adopted. Moreover, to investigate if potential differences in the results could be related to the scale parameter (μ) or to growth factor (k_T), Fig. 5a and b show the relationship (d, μ) and (T, k_T), respectively.

Annual maximum hourly precipitation by CEH-GEAR (Fig. 6c) shows values in-between 15.5 mm/h (for $T = 5$ y) and 27.7 mm/h (for $T = 100$ y). ERA5 returns a significant underestimation while ERA5@2km values are in line with those provided by CEH-GEAR. This is mainly ascribable to differences in terms of (d, μ) (Fig. 6a) and only in part to differences in terms of (T, k_T) (Fig. 6b).

3.1.2. Validation against RADKLIM-RW (2001–2017) for Cologne (DE)

Fig. 7 shows the spatial distribution of annual precipitation provided by ERA5 (Fig. 7a), ERA5@2km (Fig. 7b) and RADKLIM-RW (Fig. 7c) for Cologne (DE) over the period 2001–2017. The maps are plotted considering all the grid points belonging to the city evaluation domains in their native resolution (i.e., 15, 832, and 4712 grid points for ERA5, ERA5@2km, and RADKLIM-RW, respectively).

Both ERA5 (Fig. 7a) and ERA5@2km (Fig. 7b) well detect the spatial pattern of observed annual precipitation (Fig. 7c) with values increasing from the south-western to the north-eastern area of the domain. In general, RADKLIM-RW precipitation data provides values with a spatial average of 822 mm/y and a standard deviation of 144 mm/y. Compared to observations, ERA5 overestimates annual precipitation (spatial average = 1008 mm/y) with a similar variability (standard deviation = 152 mm/y). Conversely, ERA5@2km is able to better match annual precipitation amounts provided by gridded observations (ERA5@2km spatial average = 865 mm/y) maintaining a correct spatial variability (standard deviation = 153 mm/y).

As for the multi-year cycle of monthly precipitation (Fig. 8), RADKLIM-RW monthly precipitation ranges between 48 mm/month (April) and 90 mm/month (August).

ERA5 and ERA5@2km provide a satisfying temporal correlation with observations especially in terms of peaks timing; in terms of amplitude, ERA5 overestimation shown in Fig. 7 is also declined at the monthly scale with values ranging between 60 mm/month and 104 mm/month, while ERA5@2km adjusts these values making them in line with observations. Such an improvement is reflected by the KGE index ($KGE_{ERA5} = 0.75$ against $KGE_{ERA5@2km} = 0.88$).

Fig. 9 compares RADKLIM-RW hourly precipitation PDF to the models' ones.

The tendency is similar to the one occurring for London (UK) (see Fig. 4). Specifically, observation hourly precipitation PDF gives a tail with maximum value of $\simeq$ 10 mm/h. Compared to observations, ERA5 returns an underestimation for hourly precipitation values in the range 2–6 mm/h; conversely, ERA5@2km provides values closer to observations, with slight overestimation in-between 6-8 mm/h and a tendency to produce a longer tail ($\simeq$ 15 mm/h). Also in this case, an added value of ERA5@2km is detected (DAV = 26%).

Fig. 10 plots the multi-year cycle of hourly summer precipitation provided by RADKLIM-RW, ERA5, and ERA5@2km.

Both gridded observations and modelling show a similar trend of the diurnal cycle, with ERA5 maximizing amplitude (0.219 mm/h) in

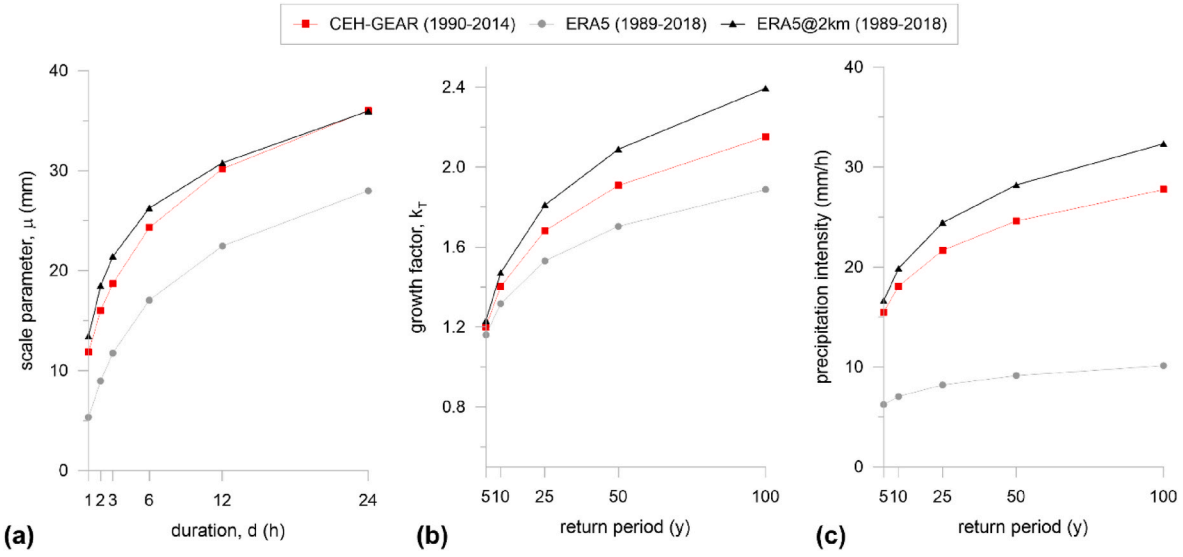

Fig. 6. Probability distribution of annual maximum extreme rainfall for London (UK) by storm-index method: (a) relationship between average annual maxima and rainfall duration; (b) growth factor for different return periods; (b) 1-hr annual maxima for different return periods.

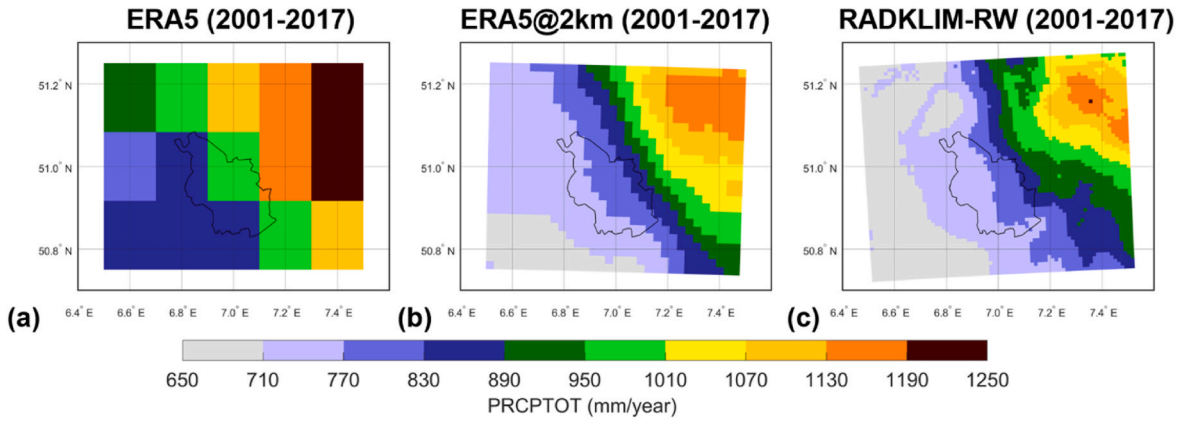

Fig. 7. Average annual precipitation over Cologne (DE) for the period 2001–2017 with different datasets: (a) ERA5 (≃ 31 km); (b) ERA5@2km (≃ 2.2 km); (c) RADKLIM-RW (≃ 1 km).

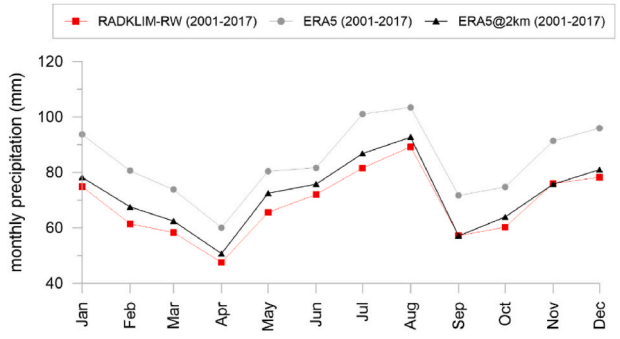

Fig. 8. Annual cycle of monthly precipitation over Cologne (DE) for the period 2001–2017 with different datasets (i.e., RADKLIM-RW, ERA5, ERA5@2km).

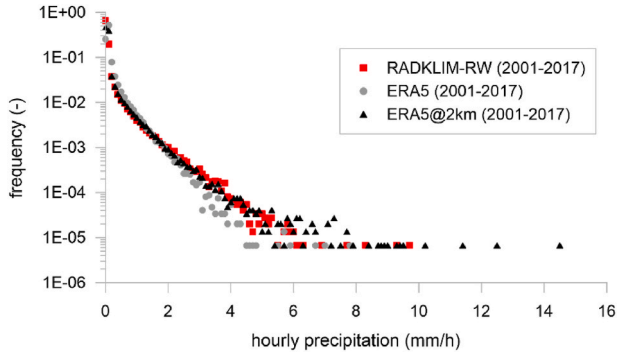

Fig. 9. Probability density function (PDF) of hourly precipitation over Cologne (DE) for the period 2001–2017 with different datasets (i.e., RADKLIM-RW, ERA5, ERA5@2km).

comparison with RADKLIM-RW (0.177 mm/h) and ERA5@2km (0.201 mm/h). The peak is delayed by 1 h for ERA5 and ERA5@2km compared to the observations (at 14UTC). In general, ERA5 tends to overestimate observations during daylight; conversely, ERA5@2km lowers observations in the range 10UTC to 13UTC while an opposite behaviour is highlighted from 14UTC to 18UTC. During night-time, both ERA5 and ERA5@2km match well with observations. In terms of KGE, ERA5@2km (KGE = 0.73) outperforms ERA5 (KGE = 0.61).

In terms of annual maximum hourly precipitation (Fig. 11), the same tendency, emerged for the previous case, arises.

RADKLIM-RW returns annual maximum hourly precipitation (Fig. 11c) ranging between 16.7 mm/h (for $T = 5$ y) and 28.4 mm/h (for

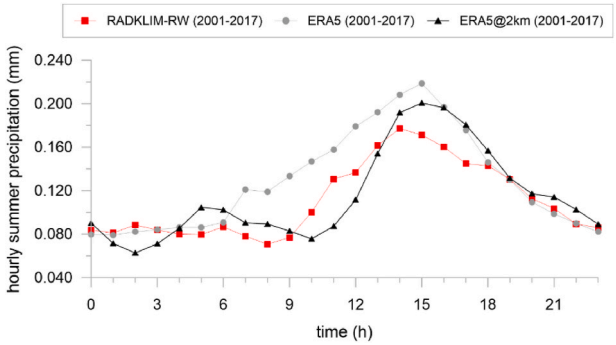

Fig. 10. Daily cycle of hourly summer precipitation over Cologne (DE) for the period 2001–2017 with different datasets (i.e., RADKLIM-RW, ERA5, ERA5@2km); time is in UTC.

$T = 100$ y). ERA5@2km yields increased values (i.e., 22.8 mm/h for $T = 5$ y and 41.3 mm/h for $T = 100$ y) in comparison with RADKLIM-RW; such a difference could be also related to the different period considered for IDF computation by RADKLIM-RW (2001–2017) and ERA5@2km (1989–2018). In line with other cases, ERA5 largely underestimates extreme hourly precipitation. For the case in hand, in terms of (d, μ) (Fig. 11a), the three datasets provide trends that are correlated but shifted for magnitude with higher values associated with ERA5@2km. In terms of (T, k_T) (Fig. 11b), ERA5@2km shows a variability similar to RADKLIM-RW and larger in comparison with ERA5.

3.1.3. *Validation against GRIPHO (2001–2016) for Milan (IT)*

Fig. 12 shows the spatial distribution of annual precipitation computed with ERA5 (Fig. 12a), ERA5@2km (Fig. 12b), and GRIPHO (Fig. 12c) for Milan (IT). For the case in hand, GRIPHO features a spatial resolution (≃ 10 km) lower than the high-resolution observational datasets used for the validation at city scale in the other cases. However, it provides hourly data enabling the computation of multi-year cycle of hourly summer precipitation and of annual maximum hourly precipitation at prescribed recurrence intervals. Moreover, it relies only on rain gauge measurements and then it is not affected by uncertainties related to the merging of local station data with radar data.

For all the following analyses, all the grid points belonging to the city evaluation domains in their native resolution (i.e., 24, 1974, and 90 grid points for ERA5, ERA5@2km, and GRIPHO, respectively) are considered.

GRIPHO precipitation data (Fig. 12c) returns values with a spatial average of 971 mm/year and a standard deviation of 217 mm/year.

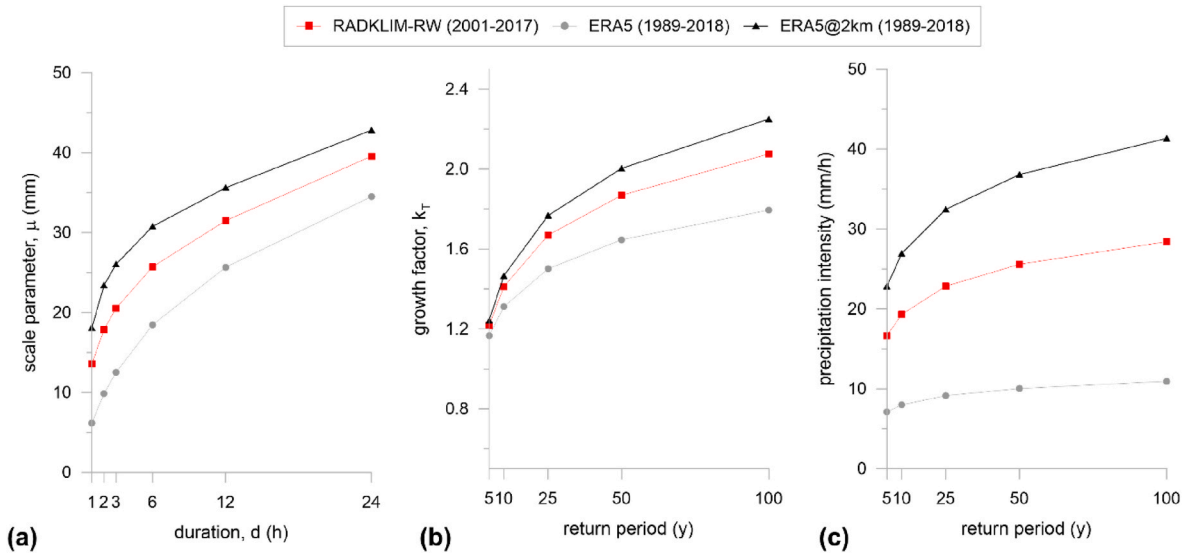

Fig. 11. Probability distribution of annual maximum extreme rainfall for Cologne (DE) by storm-index method: (a) relationship between average annual maxima and rainfall duration; (b) growth factor for different return periods; (b) 1-hr annual maxima for different return periods.

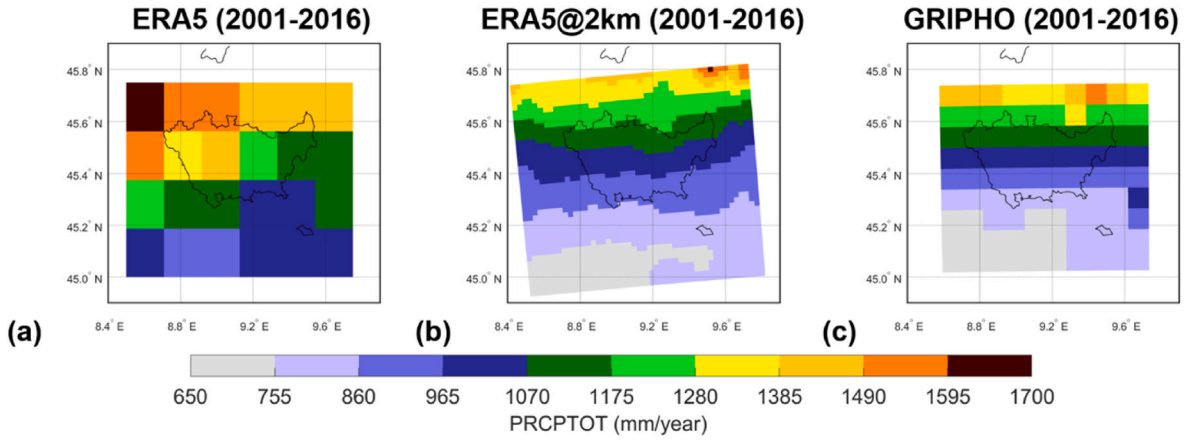

Fig. 12. Average annual precipitation over Milan (IT) for the period 2001–2016 with different datasets: (a) ERA5 (≃ 31 km); (b) ERA5@2km (≃ 2.2 km); (c) GRIPHO (≃ 10 km).

Values increase with latitude as long as the Alps are approached. Compared to GRIPHO, ERA5 (Fig. 12a) overestimates both annual precipitation (spatial average = 1221 mm/year) and related variability (standard deviation = 234 mm/year). The dynamical downscaling of ERA5 at 2 km (Fig. 12b) adjusts the spatial distribution of annual precipitation both for mean values (spatial average = 979 mm/year) and for variability (standard deviation = 209 mm/year) returning values in line with GRIPHO, also in terms of spatial pattern. Such an improvement highlights an important added value associated with ERA5@2km.

Moving to the monthly scale, Fig. 13 shows the multi-year cycle of monthly precipitation for Milan.

Observational monthly precipitation highlights values varying between 60 mm/month (July) and 140 mm/month (November). Compared to GRIPHO, ERA5 shows a well correlated trend against observations ($\rho = 0.95$) even if values are overestimated for the whole average year as pointed out for spatial distribution in Fig. 12. Localizing ERA5 precipitation at 2.2 km reduces monthly precipitation giving values in line with those returned by GRIPHO albeit ERA5@2km is not able to detect the magnitude of November peak (140 mm/month for GRIPHO against 115 mm/month for ERA5@2km). In terms of KGE index, ERA5@2km outperforms ERA5 with an improvement from 0.75 (KGE_{ERA5}) to 0.82 ($KGE_{ERA5@2km}$).

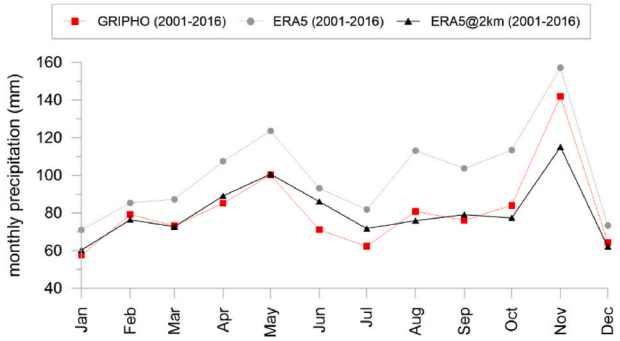

Fig. 13. Annual cycle of monthly precipitation over Milan (IT) for the period 2001–2016 with different datasets (i.e., GRIPHO, ERA5, ERA5@2km).

Moving to the hourly scale, Fig. 14 shows the PDFs of hourly precipitation provided by GRIPHO, ERA5, and ERA5@2km.

GRIPHO hourly precipitation PDF features a tail with maximum value of ≃ 19 mm/h. Compared to observations, both models' hourly precipitation PDFs detect an underestimation with a tendency to

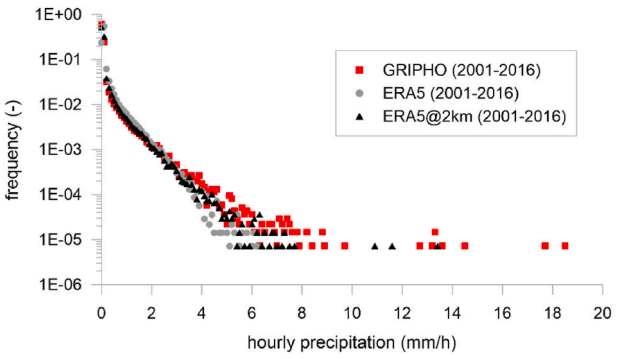

Fig. 14. Probability density function (PDF) of hourly precipitation over Milan (IT) for the period 2001–2016 with different datasets (i.e., GRIPHO, ERA5, ERA5@2km).

produce a shorter tail ($\simeq$ 5 mm/h for ERA5 and $\simeq$ 14 mm/h for ERA5@2km). Despite such an underestimation, the new VHR precipitation dataset gives an added value compared to ERA5 (DAV = 35%).

As for the multi-year cycle of hourly summer precipitation (Fig. 15), both ERA5 and ERA5@2km differ from observations.

The amplitude of the diurnal cycle for ERA5 and ERA5@2km is larger (0.194 mm/h and 0.221 mm/h, respectively) and shifted to earlier times by 3 (ERA5) and 2 (ERA5@2km) hours compared to the observations; GRIPHO is characterized by a peak of 0.152 mm/h at 19 UTC instead. ERA5 generally overestimates observations, except for the last hours of the day. It also seems to show a difference between 6UTC and 7UTC. Conversely, ERA5@2km better matches observed hourly precipitation amounts during night-time and part of daytime while in the afternoon amplitudes and phasing differ from observations. Also for this test case, in terms of KGE, ERA5@2km (KGE = 0.29) outperforms ERA5 (KGE = 0.08) even if KGE values are lower in comparison with the previous test cases.

Finally, Fig. 16 provides the annual maximum hourly precipitation computed for observations and climate simulations with the related (d, μ) and (T, k_T) relationships.

Annual maximum hourly precipitation by GRIPHO (Fig. 16c) shows values between 26.1 mm/h (for $T = 5$ y) and 50.0 mm/h (for $T = 100$ y). ERA5 returns a significant underestimation while ERA5@2km values are in line (i.e., 33.4 mm/h for $T = 5$ y and 54.7 mm/h for $T = 100$ y) with observations. ERA5@2km scale parameters (Fig. 16a) are slightly higher against GRIPHO for durations <12 h while the opposite occurs for durations >12 h. The bias between ERA5 and the observational dataset in the (d, μ) plane is limited in comparison with other test cases; moreover, for duration = 24 h, ERA5 returns a value similar to ERA5@2km. In terms of growth factors (Fig. 16b), GRIPHO points out the higher variability, even if also for the case in hand, the limited period

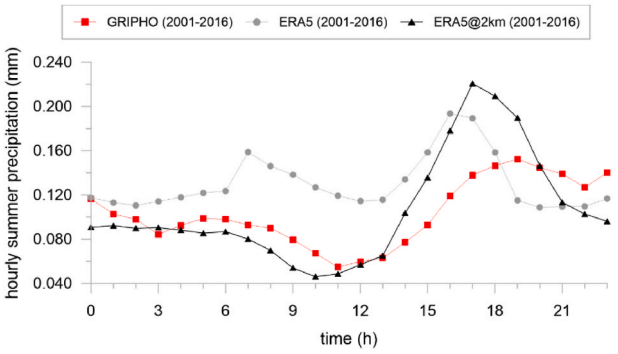

Fig. 15. Daily cycle of hourly summer precipitation over Milan (IT) for the period 2001–2016 with different datasets (i.e., GRIPHO, ERA5, ERA5@2km); time is in UTC.

for IDF computation (2001–2016) should be properly accounted for.

3.1.4. Some insights about differences in IDF curves

Analysis against high-resolution observational datasets have shown how ERA5 lowers annual maximum hourly precipitation at different return times even if it overestimates precipitation patterns at yearly, monthly and daily scales. Downscaling ERA5 at CP scale instead moderates ERA5 overestimations resulting also in annual maximum hourly precipitation in line with observations.

The aim of this section is to further investigate the differences in annual maximum hourly precipitation. In general, the performed analysis reflects the coarser resolution of ERA5 ($\simeq$31 km) data in comparison with ERA5@2km ($\simeq$2.2 km) and high-resolution observations ($\simeq$1 km for CEH-GEAR, and RADKLIM-RW; $\simeq$10 km for GRIPHO). ERA5 resolution implies that each grid point is informative for an area, at least, equal to 31 $\times$ 31 km^2, and then, for each grid cell, weather variables (e.g., for precipitation as verified in different works, e.g., Reder and Rianna, 2021) can be affected in their magnitude by an averaging effect which produces a smoothing especially for maximum precipitation values. Such a smoothing effect decreases with spatial resolution enhancement.

However, as all data have been processed on their native grids, it is not possible to quantify the interplayed effects of spatial resolution and informative contents provided by each dataset. For this reason, it is necessary to limit these effects by neglecting one of both. To do this, in this section annual maximum hourly precipitation are computed by interpolating ERA5@2km data and observations onto ERA5 grids, to set a common spatial resolution.

Before that, in Fig. 17 the values of hourly precipitation obtained considering observations and ERA5@2km onto native grids are compared with those computed upscaling data onto the common ERA5 grids. Operatively, native data and interpolated ones are first averaged over each city evaluation domain and then represented.

Such a comparison shows that avoiding spatial upscaling onto common grids exerted a minor and negligible effect on the findings carried out during the evaluation of ERA5@2km, as points fall around the 1:1 line for almost all the cases with R squared coefficients in general higher than 0.92. This means that the finding introduced in the previous section would also be valid if the investigation had been carried out on a shared grid.

By looking at extreme hourly precipitation, Fig. 18 and Fig. 19 compare for each test case the scale parameters (μ) for different durations (d) and the growth factors (k_T) for different return periods (T) obtained considering native grids with those computed considering the common ERA5 grids.

Interpolating data on a coarser grid does not alter the informative contents given by ERA5@2km and observations as points fall across the 1:1 line for almost all the cases. This makes evidence of the added value of a VHR reanalysis-based climate simulation in comparison with ERA5 for extreme values, giving us a high degree of confidence in the quality of the downscaling activity performed and in the reliability of IDF data produced (see Annex B).

3.2. Validation against E-OBS data

The last section of this work provides a general evaluation framework for all the 20 European cities considered for the downscaling activity of ERA5 at ~2.2 km. In this perspective, as no unique high-resolution gridded observational dataset covering all the test cases is available, daily precipitation data provided by E-OBS are assumed as reference. Moreover, ERA5 data are also considered to determine potential gains and losses due to the dynamical localization of parent ERA5 reanalysis upon a finer grid.

To simplify the data analysis, in this section a bird's eye view is provided by analysing for each city the PDFs of observed and modelled daily precipitation. Such an analysis relies on the use of DAV (see §2.3), a

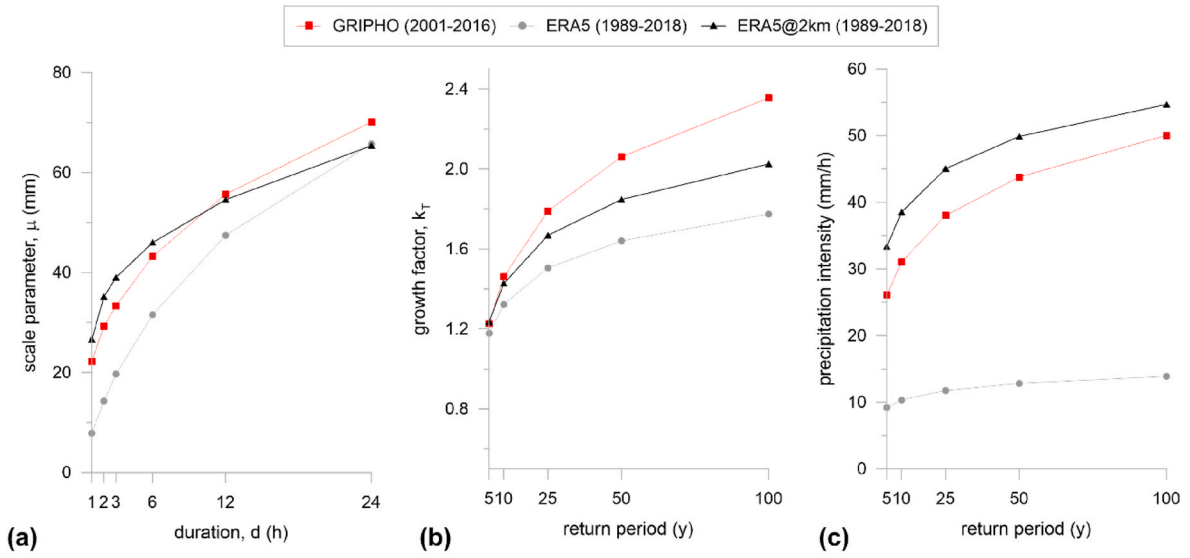

Fig. 16. Probability distribution of annual maximum extreme rainfall for Milan (IT) by storm-index method: (a) relationship between average annual maxima and rainfall duration; (b) growth factor for different return periods; (b) 1-hr annual maxima for different return periods.

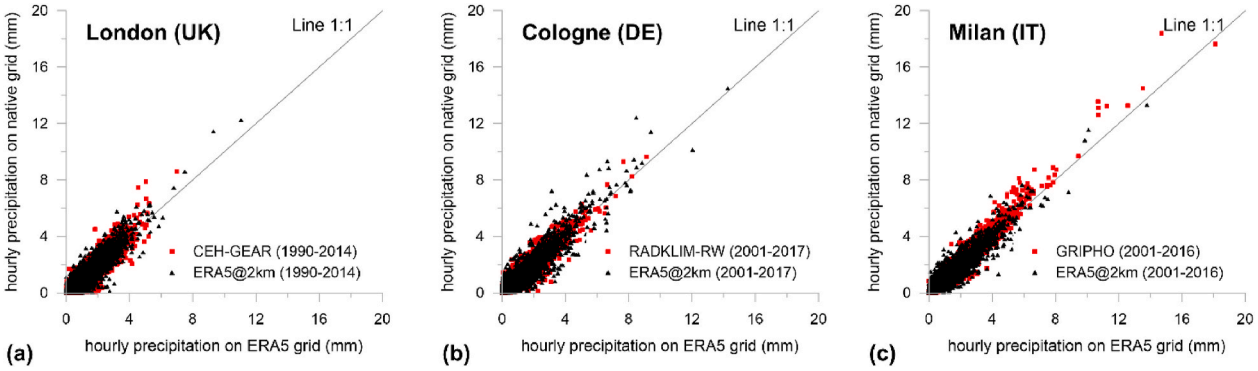

Fig. 17. Hourly precipitation for the three test cases (London, Cologne, and Milan) computed considering data on native grids and data interpolated onto a common ERA5 grid.

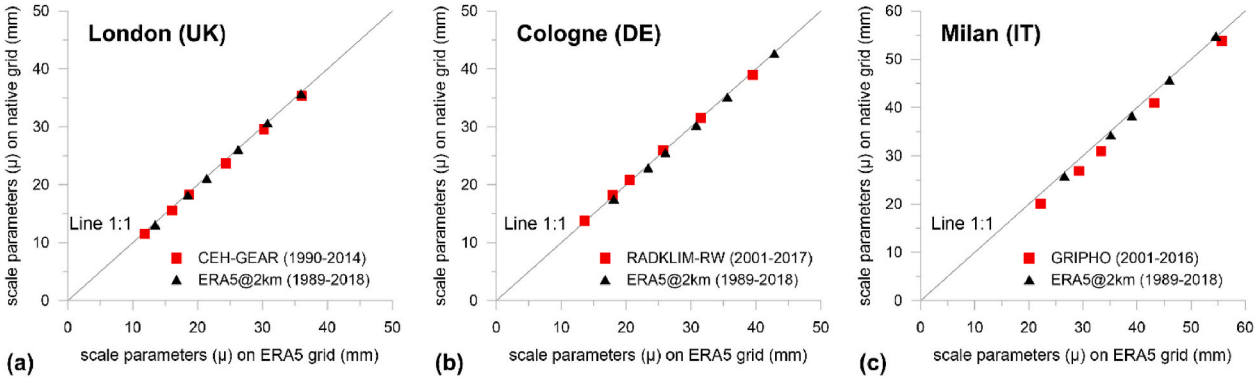

Fig. 18. Average annual maxima at different rainfall duration for the three test cases (London, Cologne, and Milan) computed considering data on native grids and data interpolated onto a common ERA5 grid.

metric which is able to estimate potential gains and losses when moving from coarser (ERA5) to finer (ERA5@2km) resolutions. A further detail for each city is reported in Annex A which depicts spatial distribution of annual precipitation provided by E-OBS, ERA5, and ERA5@2km as well as the multi-year cycle of monthly precipitation and the annual maximum daily precipitation at prescribed return periods, including also data relying on ECA&D station network.

The results of this analysis for the different cities handled in this study are summarized in Fig. 20.

They highlight a general added value in moving from ERA5 to ERA5@2km, as already outlined by evaluation with high-resolution observations performed in the previous sections. Such a tendency is highlighted for 90% (18 out of 20) of investigated cities. In general, DAV varies in the range 10–20% reaching in some cases also values of

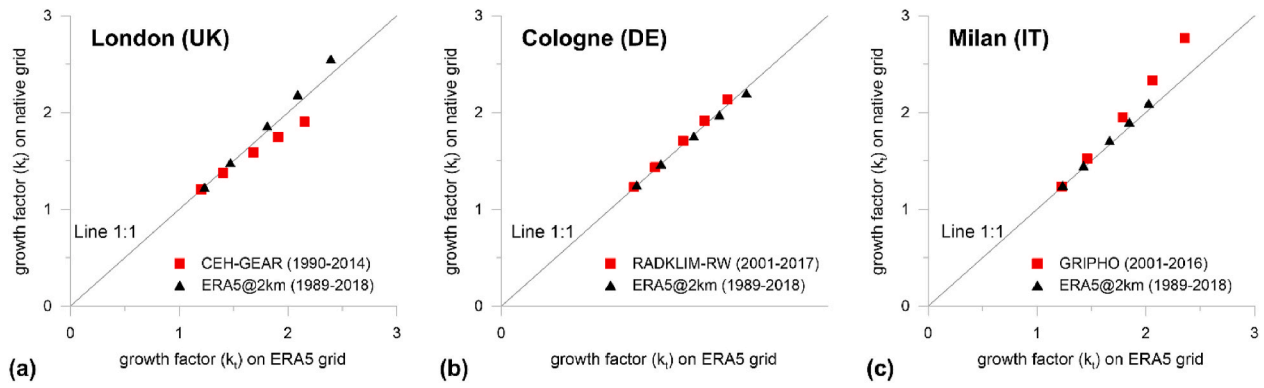

Fig. 19. Growth factor for different return periods for the three test cases (London, Cologne, and Milan) computed considering data on native grids and data interpolated onto a common ERA5 grid.

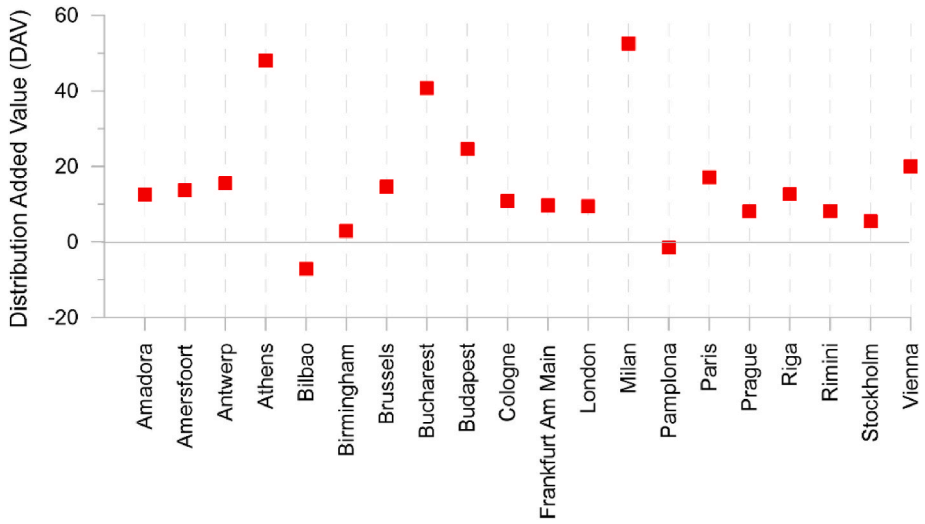

Fig. 20. Distribution Added Value (DAV) estimated for the pool of European cities for which ERA5@2km precipitation data are produced. DAV is computed from the probability density function (PDF) of daily precipitation by assuming ERA5@2km as finer model, ERA5 as coarser model, and E-OBS as reference for observations.

40–50%. Some constrains and uncertainties in ERA5@2km accuracy may arise for those cities located in areas characterized by peculiar circulation patterns (e.g., for those cities for example Bilbao and Pamplona where the lateral boundaries are mainly regulated by the Atlantic Sea, and CCLM is not able to reproduce these dynamics as it is uncoupled from an ocean model). Such an issue has also been investigated by extending the computational domain. However, the improvement associated with such an extension is not so evident in capturing all lateral dynamics and, moreover, it does not comply with time and computational requirements.

Finally, it should also be emphasized how validation could be affected by the reliability of E-OBS data which mainly depends on the availability for a specific city of local station data in the ECA&D network forming the base for E-OBS gridded observations. Further details in this sense can be retrieved in Cornes et al. (2018). As an instance, the reliability is higher for cities located in Germany, Northern Italy, and Sweden whereas it is reduced in other countries such as Greece or Hungary.

4. Conclusions

The availability of reliable spatial and temporal data at proper spatial and temporal scale about extreme weather events represents a pivotal challenge for supporting DRR policy and practice. On this issue, the recent advent of CP-RCMs is providing a step change in the capability for modelling past climate and future climate change at local scales, especially for extreme weather events that most impact society (Kendon et al., 2021). This includes the opportunity of providing credible data for short-duration precipitation extremes, partly matching the expected spatial and temporal requirements of impact analysis at city scale.

Based on this state-of-the-art, a new high-resolution hourly precipitation dataset, ERA5@2km, for the past thirty years (1989–2018) has been made available by dynamically downscaling ERA5 at CP scale (i.e., at 0.02°, 2.2 km) over a set of 20 European cities, with the ambition of providing a basis for impact analysis at city scale, in terms of extreme hourly precipitation for different return times (data are reported as Supplementary Material in Annex B).

This work evaluates the reliability of this new precipitation dataset for spatial patterns, trends, and extreme values. The evaluation is performed by making use of a set of available high-resolution observational datasets (comparable in terms of spatial and temporal resolution) for a subset of cities (i.e., London, Cologne, and Milan). Moreover, to provide a general evaluation across the whole set of cities, a further evaluation has been developed against daily E-OBS precipitation data.

The evaluation activity provides a clearer understanding about the added value of ERA5@2km in terms of localization and magnitude of precipitation events at urban scale confirming a general and relevant added value of this new configuration for the assessment for extreme atmospheric events (such as heavy precipitations). Such an

enhancement has been highlighted by comparing ERA5@2km data with high-resolution hourly observations and ERA5 data, analysing multiple features of interest such as mean spatial pattern of annual precipitation, multi-year cycle of monthly precipitation, multi-year cycle of hourly precipitation for summer season, and annual maximum hourly precipitation at prescribed recurrence intervals.

ERA5 represents a good reference for general mean statistics (e.g., spatial pattern of annual precipitation, multi-year cycle of monthly precipitation); however, its coarser resolution tends to generate a smoothing of extreme precipitation, confirming the need of highly localized data. ERA5@2km overcomes this constraint by providing a reliable suite of extreme precipitation values for city analyses. Such an expected increase in performances can justify the required investment in time and computational resources, especially in those areas where either consolidated institutional IDF curves are not available or local observations are not sufficient (for temporal coverage, temporal resolution, and spatial resolution) to provide an estimation of extreme precipitation values. In this sense, further work will certainly be needed to characterise sub-daily precipitation patterns and to further improve the reliability of CPMs as also noted in Fowler et al. (2021).

A climate dataset such as ERA5@2km may also be a relevant tool to support adaptation strategies and risk assessment. Such a relevance is mainly related to the large number of atmospheric variables and, subsequently, of climate indices and indicators, that can be evaluated with a level of significance and reliability larger than allowed by the usually limited temporal coverage of in-situ atmospheric variables. Reanalysis (-based) datasets can indeed fill observational gaps, still existing in wide areas, especially if different reanalysis datasets are available for evaluating the local uncertainty associated to their estimations. Additionally, the large amount of model outputs features allow including in impact models those atmospheric variables for which monitoring networks are still poor. Finally, VHR reanalysis (-based) data can support risk assessment as well as adaptation analysis at local scale.

Declaration of competing interest

The authors declare that they have no known competing financial interests or personal relationships that could have appeared to influence the work reported in this paper.

Acknowledgments

Part of the activities described in this paper have been funded by the Copernicus Climate Change Service. ECMWF implements the Copernicus Climate Change Service and the Copernicus Atmosphere Monitoring Service on behalf of the European Commission. The experiments have been performed using the COSMO model in CLimate Mode (COSMO-CLM). COSMO-CLM is the community model of the German regional climate re-search jointly further developed by the CLM-Community. We acknowledge the members of the community for their common efforts to develop the model and to find right setups.

ERA5 data have been generated using Copernicus Climate Change Service Information and downloaded from the C3S CDS.

The authors are grateful to DWD for providing open access RADKLIM-RW data, and to UK Centre for Ecology & Hydrology for providing the access to CEH-GEAR data. They would thank Emanuela Pichelli and Erika Coppola from UNESCO ICTP for allowing access to the Italian database of precipitation GRIPHO. Finally, we acknowledge the E-OBS dataset from the EU-FP6 project UERRA (http://www.uerra.eu) and the Copernicus Climate Change Service, and the data providers in the ECA&D project (https://www.ecad.eu).

Appendix A. Supplementary data

Supplementary data to this article can be found online at https://doi.org/10.1016/j.wace.2022.100407.

References

Adinolfi, M., Raffa, M., Reder, A., Mercogliano, P., 2021. Evaluation and expected changes of summer precipitation at convection permitting scale with COSMO-CLM over Alpine space. Atmosphere 12, 54. https://doi.org/10.3390/atmos12010054-.

Anderson, T.W., Darling, D.A., 1954. A test of goodness of fit. J. Am. Stat. Assoc. 49 (268), 765–769. https://doi.org/10.1080/01621459.1954.10501232.

Baldauf, M., Schulz, J.P., 2004. Prognostic precipitation in the lokal modell (LM) of DWD. COSMO Newsletter No. 4.; Deutscher Wetterdienst: Offenbach am Main, Germany, pp. 177–180.

Ban, N., Caillaud, C., Coppola, E., Mercogliano, et al., 2021. The first multi-model ensemble of regional climate simulations at kilometer-scale resolution, part I: evaluation of precipitation. Clim. Dynam. https://doi.org/10.1007/s00382-021-05708-w.

Ban, N., Schmidli, J., Schär, C., 2014. Evaluation of the new convective-resolving regional climate modelling approach in decade-long simulations. J. Geophys. Res. Atmos. 119, 7889–7907. https://doi.org/10.1002/2014JD021478.

Bartholomé, E., Belward, A.S., 2005. GLC2000; a new approach to global land cover mapping from earth observation data. Int. J. Rem. Sens. 26, 1959–1977.

Berthou, S., Kendon, E.J., Chan, S.C., Ban, N., Leutwyler, D., Schär, C., Fosser, G., 2018. Pan-European climate at convection-permitting scale: a model intercomparison study. Clim. Dynam. 5, 1–25. https://doi.org/10.1007/s00382-018-4114-6.

Buontempo, C., Hutjes, R., Beavis, P., Berckmans, J., Cagnazzo, C., Vamborg, F., Thépaut, J.N., Bergeron, C., Almond, S., Amici, A., Ramasamy, S., Dee, D., 2020. Fostering the development of climate services through Copernicus climate change service (C3S) for agricultural applications. Weather Clim. Extrem. 27, 100226 https://doi.org/10.1016/j.wace.2019.100226.

Caporali, E., Cavigli, E., Petrucci, A., 2008. The index rainfall in the regional frequency analysis of extreme events in Tuscany (Italy). Environmetrics 19 (7), 714–724.

Chow, V.T., Maidment, D.R., Mays, L.W., 1988. Applied Hydrology. McGraw-Hill.

Coppola, E., Sobolowski, S., Pichelli, E., et al., 2020. A first-of-its-kind multi-model convection permitting ensemble for investigating convective phenomena over Europe and the Mediterranean. Clim. Dynam. 55, 3–34. https://doi.org/10.1007/s00382-018-4521-8.

Cornes, R., van der Schrier, G., van den Besselaar, E.J.M., Jones, P.D., 2018. An ensemble version of the E-OBS temperature and precipitation datasets. J. Geophys. Res. Atmos. 123, 9391–9409. https://doi.org/10.1029/2017JD028200.

Dee, D.P., et al., 2011. The ERA-Interim reanalysis: configuration and performance of the data assimilation system. Q. J. R. Meteorol. Soc. 137 (656), 553–597.

Desiato, F., Fioravanti, G., Fraschetti, P., Perconti, W., Toreti, A., 2011. Climate indicators for Italy: calculation and dissemination. Adv. Sci. Res. 6, 147–150.

Doms, G., Forstner, J., Heise, E., Herzog, H.J., Mironov, D., Raschendorfer, T., Reinhardt, T., Ritter, B., Schrodin, R., Schulz, J.P., et al., 2011. A Description of the Non-hydrostatic Regional COSMO Model. Part-II: Physical Parameterization. Available online: https://klimanavigator.eu/imperia/md/content/csc/klimanavigator/cosmophysparamtr.pdf. (Accessed 23 December 2020).

Fantini, A., 2019. Climate Change Impact on Ood Hazard over Italy. Ph.D. Thesis. Universita degli Studi di Trieste, Trieste, Italy.

Fosser, G., Khodayar, S., Berg, P., 2015. Benefit of convection permitting climate model simulations in the representation of convective precipitation. Clim. Dynam. 44 (1–2), 45–60. https://doi.org/10.1007/s00382-014-2242-1.

Fowler, H.J., Wasko, C., Prein, A.F., 2021. Intensification of short-duration rainfall extremes and implications for flood risk: current state of the art and future directions. Phil. Trans. R. Soc. A 379, 20190541. https://doi.org/10.1098/rsta.2019.0541.

Frick, C., Steiner, H., Mazurkiewicz, A., Riediger, U., Rauthe, M., Reich, T., Gratzki, A., 2014. Central European high-resolution gridded daily data sets (HYRAS): mean temperature and relative humidity. Meteorol. Z. 23, 15–32. https://doi.org/10.1127/0941-2948/2014/0560.

Fumière, Q., Déqué, M., Nuissier, O., Somot, S., Alias, A., Caillaud, C., Laurantin, O., Seity, Y., 2020. Extreme rainfall in Mediterranean France during the fall: added-value of the CNRM-AROME convection permitting regional climate model. Clim. Dynam. 55, 77–91. https://doi.org/10.1007/s00382-019-04898-8.

Giorgi, F., Gutowski, W.J., 2015. Regional dynamical downscaling and the CORDEX initiative. Annu. Rev. Environ. Resour. 40, 467–490.

Gupta, H.V., Kling, H., Yilmaz, K.K., Martinez, G.F., 2009. Decomposition of the mean squared error and NSE performance criteria: implications for improving hydrological modelling. J. Hydrol. 377, 80–91.

Haylock, M.R., Hofstra, N., Klein Tank, A.M.G., Klok, E.J., Jones, P.D., New, M., 2008. A European daily high-resolution gridded data set of surface temperature and precipitation for 1950–2006. J. Geophys. Res. Atmos. 113.

Herrera, S., Cardoso, R.M., Soares, P.M., Espírito-Santo, F., Viterbo, P., Gutiérrez, J.M., 2019. Iberia01: a new gridded dataset of daily precipitation and temperatures over Iberia. Earth Syst. Sci. Data 11, 1947–1956. https://doi.org/10.5194/essd-11-1947-2019.

Hersbach, H., Bell, B., Berrisford, P., Hirahara, S., et al., 2020. The ERA5 global reanalysis. Q. J. R. Meteorol. Soc. 146 (730), 1999–2049. https://doi.org/10.1002/qj.3803.

Hosking, J.R.M., Wallis, J.R., Wood, E.F., 1985. Estimation of the generalized extreme-value distribution by the method of probability weighted moments. Technometrics 27 (3), 251–261. https://doi.org/10.1080/00401706.1985.10488049.

Isotta, F., Frei, C., Weilguni, V., Tadic, M.P., Lassegues, P., Rudolf, B., Pavan, V., Cacciamani, C., Antolini, G., Ratto, S.M., et al., 2014. The climate of daily precipitation in the Alps: development and analysis of a high-resolution grid dataset from pan-Alpine rain-gauge data. Int. J. Climatol. 34, 1657–1675.

Jacob, D., Petersen, J., Eggert, B., Alias, A., Christensen, O.B., Bouwer, L.M., Braun, A., Colette, A., Deque, M., Georgievski, G., et al., 2014. EURO-CORDEX: new high-resolution climate change projections for European impact research. Reg. Environ. Change 14, 563–578.

Kendon, E.J., Prein, A.F., Senior, C.A., Stirling, A., 2021. Challenges and outlook for convection-permitting climate modelling. Phil. Trans. R. Soc. A. https://doi.org/10.1098/rsta.2019.0547, 3792019054720190547.

Knoben, W.J.M., Freer, J.E., Woods, R.A., 2019. Technical note: inherent benchmark or not? Comparing Nash–Sutcliffe and Kling–Gupta efficiency scores. Hydrol. Earth Syst. Sci. 23, 4323–4331.

Kottegoda, N.T., Rosso, R., 2008. Applied Statistics for Civil and Environmental Engineers, second ed. John Wiley and Sons, UK.

Lewis, E., Quinn, N., Blenkinsop, S., Fowler, H.J., Freer, J., Tanguy, M., Hitt, O., Coxon, G., Bates, P., Woods, R., 2019. Gridded Estimates of Hourly Areal Rainfall for Great Britain (1990-2014). [CEH-GEAR1hr], NERC Environmental Information Data Centre. https://doi.org/10.5285/d4ddc781-25f3-423a-bba0-747cc82dc6fa.

Lussana, C., Saloranta, T., Skaugen, T., Magnusson, J., Tveito, O.E., Andersen, J., 2018. seNorge2 daily precipitation, an observational gridded dataset over Norway from 1957 to the present day. Earth Syst. Sci. Data 10, 235–249. https://doi.org/10.5194/essd-10-235-2018. https://www.earth-syst-sci-data.net/10/235/2018/.

Madsen, H., Gregersen, I.B., Rosbjerg, D., Arnbjerg-Nielsen, K., 2017. Regional frequency analysis of short duration rainfall extremes using gridded daily rainfall data as co-variate. Water Sci. Technol. 75 (8), 1971–1981.

Mellor, G.L., Yamada, T., 1982. Development of a turbulence closure model for geophysical fluid problems. Rev. Geophys. 20, 851–875. https://doi.org/10.1029/RG020i004p00851.

Mercogliano, P., Rianna, G., Reder, A., Raffa, M., Mancini, M., Stojiljkovic, M., de Valk, C., van der Schrier, G., 2021. Extreme precipitation risk indicators for Europe and European cities from 1950 to 2019. In: Copernicus Climate Change Service (C3S) Climate Data Store (CDS). https://doi.org/10.24381/cds.3a9c4f89. (Accessed 23 September 2021).

MeteoSwiss, 2013a. Documentation of MeteoSwiss grid-data products. In: Daily Mean, Minimum and Maximum Temperature: TabsD, TminD, TmaxD, Tech. rep., Federal Office of Meteorology and Climatology MeteoSwiss, Federal Department of Home Affairs FDHA, Switzer land. https://www.meteoswiss.admin.ch/content/dam/meteoswiss/de/service-und-publikationen/produkt/raeumliche-daten-temperatur/doc/ProdDoc_TabsD.pdf.

MeteoSwiss, 2013b. Documentation of MeteoSwiss grid-data products: daily precipitation (final analysis). In: RhiresD, Tech. rep., Federal Office of Meteorology and Climatology MeteoSwiss. Federal Department of Home Affairs FDHA, Switzerland. https://www.meteoswiss.admin.ch/content/dam/meteoswiss/de/service-und-publikationen/produkt/raeumliche-daten-niederschlag/doc/ProdDoc_RhiresD.pdf.

Muñoz-Sabater, J., Dutra, E., Agustí-Panareda, A., Albergel, C., Arduini, G., Balsamo, G., Boussetta, S., Choulga, M., Harrigan, S., Hersbach, H., Martens, B., Miralles, D.G., Piles, M., Rodríguez-Fernández, N.J., Zsoter, E., Buontempo, C., Thépaut, J.-N., 2021. ERA5-Land: a state-of-the-art global reanalysis dataset for land applications [preprint] Earth Syst. Sci. Data Discuss.. https://doi.org/10.5194/essd-2021-82. in review.

Padulano, R., Reder, A., Rianna, G., 2019. An ensemble approach for the analysis of extreme rainfall under climate change in Naples (Italy). Hydrol. Process. 33 (14), 2020–2036. https://doi.org/10.1002/hyp.13449, 2019.

Piazza, M., Prein, A., Truhetz, H., Csaki, A., 2019. On the sensitivity of precipitation in convection-permitting climate simulations in the Eastern Alpine region. Meteorol. Z. 28 (4), 323–346. https://doi.org/10.1127/metz/2019/0941.

Prein, A.F., Langhans, W., Fosser, G., Ferrone, A., Ban, N., Goergen, K., et al., 2015. A review on regional convection-permitting climate modeling: demonstrations, prospects, and challenges. Rev. Geophys. 53 (2), 323–361. https://doi.org/10.1002/2014RG000475.

Raffa, M., Reder, A., Adinolfi, M., Mercogliano, P. A Comparison between One-step and Two-step Nesting Strategy in the Dynamical Downscaling of Regional Climate Model COSMO-CLM at 2.2 Km Driven by ERA5 Reanalysis. Atmosphere, under review.

Rauthe, M., Steiner, H., Riediger, U., Mazurkiewicz, A., Gratzki, A., 2013. A Central European precipitation climatology ? Part I: generation and validation of a high-resolution gridded daily data set (HYRAS). Meteorol. Z. 22, 235–256. https://doi.org/10.1127/0941-2948/2013/0436. https://doi.org/10.1127/0941-2948/2013/0436.

Reder, A., Raffa, M., Montesarchio, M., Mercogliano, P., 2020. Performance evaluation of regional climate model simulations at different spatial and temporal scales over the complex orography area of the Alpine region. Nat. Hazards 102, 151–177. https://doi.org/10.1007/s11069-020-03916-x.

Reder, A., Rianna, G., 2021. Exploring ERA5 Reanalysis Potentialities for Supporting Landslide Investigations: A Test Case from Campania Region (Southern Italy). Landslides.

Ridal, M., Olsson, E., Unden, P., Zimmermann, K., Ohlsson, A., 2017. Uncertainties in ensembles of regional Re-analyses. In: Deliv-erable D2.7 HARMONIE Reanalysis Report of Results and Dataset. Available online: http://www.uerra.eu/component/dpattachments/?task=attachment.download&id=296.

Ritter, B., Geleyn, J.F., 1992. A comprehensive radiation scheme for numerical weather prediction models with potential applications in climate simulations. Mon. Weather Rev. 120, 303–325. https://doi.org/10.1175/1520-0493(1992)120,0303:ACRSFN.2.0.CO,2.

Rockel, B., Will, A., Hence, A., 2008. The regional climate model COSMO-CLM (CCLM). Meteorol. Z. 17, 347–348. https://doi.org/10.1127/0941-2948/2008/0309.

Soares, P.M.M., Cardoso, R.M., 2017. A simple method to assess the added value using high-resolution climate distributions: application to the EURO-CORDEX daily precipitation. Int. J. Climatol. https://doi.org/10.1002/joc.5261.

Street, R., Buontempo, C., Mysiak, J., Karali, E., Pulquério, M., Murray, V., et al., 2019. How could climate services support disaster risk reduction inthe21st century. Int. J. Disaster Risk Reduc. 34, 28–33. https://doi.org/10.1016/j.ijdrr.2018.12.001.

Tabary, P., Dupuy, P., L'Hena, G., Gueguen, C., Moulin, L., Laurantin, O., Merlier, C., Soubeyroux, J.M., 2012. A 10-Year (1997–2006) Reanalysis of Quantitative Precipitation Estimation over France: Methodology and First Results, vol. 351. IAHS, Wallingford, UK, pp. 255–260.

Tiedtke, M., 1989. A comprehensive mass flux scheme for cumulus parameterization in large-scale models. Mon. Weather Rev. 117, 1779–1800. https://doi.org/10.1175/1520-0493(1989)117<1779:ACMFSF>2.0.CO,2.

Vidal, J.-P., Martin, E., Franchisteguy, L., Baillon, M., Soubeyroux, J.-M., 2010. A 50-year high-resolution atmospheric reanalysis over France with the Safran system. Int. J. Climatol. 30, 1627–1644. https://doi.org/10.1002/joc.2003. https://rmets.onlinelibrary.wiley.com/doi/abs/10.1002/joc.2003.

Viglione, A., Laio, F., Claps, P., 2007. A comparison of homogeneity tests for regional frequency analysis. Water Resour. Res. 43, W03428.

Wallis, J.R., Schaefer, M.G., Barker, B.L., Taylor, G.H., 2007. Regional precipitation-frequency analysis and spatial mapping for 24-hour and 2-hour durations for Washington State. Hydrol. Earth Syst. Sci. 11 (1), 415–442.

Winterrath, T., Brendel, C., Hafer, M., Junghänel, T., Klameth, A., Lengfeld, K., Walawender, E., Weigl, E., Becker, A., 2018. RADKLIM Version 2017.002: reprocessed gauge-adjusted radar data, one-hour precipitation sums (RW). In: Dtsch. Wetterd., p. 2.

Wouters, H., Demuzere, M., Blahak, U., Fortuniak, K., Maiheu, B., Camps, J., Tielemans, D., van Lipzig, N.P.M., 2016. The efficient urban canopy dependency parametrization (SURY) v1.0 for atmospheric modelling: description and application with the COSMO-CLM model for a Belgian summer. Geosci. Model Dev. (GMD) 9 (9), 3027–3054. https://doi.org/10.5194/gmd-9-3027-2016.